CHAPTER 8

Molecular Force Parameters through Thermal Diffusion to Ensure the Model Independency of Column Calibration Factor

Molecular Force Parameters through Thermal Diffusion to Ensure the Model Independency of Column Calibration Factor

8.1. Introduction

The theoretical formulation of thermal diffusion factor α_T as derived from Chapman-Enskog gas kinetic theory[1] is based on the assumption that the molecules are elastic spheres with spherically symmetric potential field. The theory can, however, hardly explain the experimental α_T of binary nonisotopic or even isotopic gas mixtures. Thermal diffusion is still interesting for its close correlation with the intermolecular forces. Moreover, unlike viscosity, thermal diffusion is a second order effect. Thus it is generally used to investigate the elastic or inelastic collisions among the molecules. The phenomenon is also responsible to enrich rare as well as ordinary isotopes in thermal diffusion column.

The temperature dependence of experimental α_T's of a binary gas mixture may offer a convenient method to estimate the molecular force parameters like ε_{ij}/k and σ_{ij} where ε_{ij} is the depth of potential well, k is the Boltzmann constant and σ_{ij} is the molecular diameter. ε_{ij}/k and σ_{ij} become ε_{ii}/k or ε_{jj}/k and σ_{ii} or σ_{jj} for isotopic components in a binary mixture of gases. They are, therefore, expected to play an important role to yield the exact theoretical α_T's based on elastic or inelastic collisions.

To estimate experimental α_T the theory of TD column which was already developed by a large number of workers[2-4] is still insufficient. TD column, on the other hand, is a very sensitive instrument to investigate the temperature and composition dependence of α_T particularly for a binary isotopic gas mixture of molecules having practically no mass difference.

The equilibrium separation factor of a gas mixture in a TD column is defined by :

$$q_e = (x_i/x_j)_{top} / (x_i/x_j)_{bottom}$$

where x_i and x_j are the mass or mole fractions of the lighter (i) and heavier (j) components respectively. In a TD column q_e is usually measured at different pressure in atmosphere, for a fixed composition of a binary gas mixture at different temperatures or at a fixed temperature for different compositions. The existing method of evaluating the experimental α_T is involved with Maxwell, Lennard-Jones model dependent as well as Slieker model independent column shape factors (CSF). The method is, however, complicated and the resulting α_T's usually not in agreement with the theoretical α_T's so far its temperature and composition dependences are concerned.

We [5-7] therefore, introduce a scaling factor F_s called CCF for a TD column to get the actual α_T of a binary gas mixture from column measurements by the following relation:

$$\ln q_{max} = \alpha_T F_s (r_c, r_h, L, \bar{T}). \quad \text{..... (8.1)}$$

Here $\ln q_{max}$ is the logarithmic maximum equilibrium separation factor, r_c and r_h are the cold and hot wall radii maintained at temperatures T_c and T_h respectively in a TD column of geometrical length L and the mean temperature $\bar{T}$ of the gas mixture is given by $\bar{T} = (T_h+T_c)/2$.

The molecular model independent parameter[7,8] F_s can now be used to evaluate the actual α_T's of binary isotopic or nonisotopic gas mixtures from their $\ln q_{max}$ measurements. Moran and Watson[9] had already measured the pressure dependence of $\ln q_e$ of Ne^{20}-Ne^{22}, Ar^{36}-Ar^{40}, and Kr^{80}-Kr^{86} mixtures at two experimental temperatures in a TD column of L=182.0 cm, r_c=0.635 cm and r_h=0.0254 cm respectively. The measurements[9], however, inspired us to observe the probable temperature dependence of α_T of those isotopic mixtures in terms of CCF together with the estimation of ε_{ij}/k and σ_{ij} of the respective molecules. The purpose of such study is to establish the molecular model independency of F_s too.

The experimental[9] $\ln q_{max}$ of Ar^{36}-Ar^{40} at 432K and 537K and the reliable[10] α_T's of Ar were, however, used to give two values of F_s. As F_s is a molecular model independent parameter, the experimental[9] $\ln q_{max}$ and reliable[10] α_T of

Ne^{20}-Ne^{22} were used again to get F_s at the intermediate temperature 447K. The probable temperature dependence of F_s for the column[9] is then obtained

$$F_s = 54.3777 - 0.1152\bar{T} + 1.4350 \times 10^{-4}\bar{T}^2 \quad \text{..... (8.2)}$$

which is shown graphically in Fig. 8.1. This F_s and the experimental $\ln q_{max}$ for any gas mixture yield α_T at the experimental temperature $\bar{T}$ from eq. (8.1).

A large number of workers[11,12] had expressed α_T in the form :

$$\alpha_T = A + B / \bar{T} \quad \text{..... (8.3)}$$

where A and B are two arbitrary constants. The experimental α_T's for Ne^{20}-Ne^{22}, Ar^{36}-Ar^{40} and Kr^{80}-Kr^{86} as a function of $\bar{T}$ are, however given by

$$\alpha_T = 0.03019 - 0.80013 / \bar{T},$$

$$\alpha_T = 0.03476 - 5.08155 / \bar{T} \text{ and} \quad \text{..... (8.4)}$$

$$\alpha_T = 0.27993 - 69.3446 / \bar{T}$$

which are shown in Figs. 8.3-8.5 respectively. The plot of experimental α_T's against $\bar{T}$ thus enables us to evaluate ε_{ij}/k and σ_{ij} of the respective molecules[13,14]. The results are shown in Table 8.2 for comparison with the literature values. The comparison finally indicates that curves as shown in Figs. 8.3-8.5 in terms of F_s and $\ln q_{max}$ from eq (8.1) for Ne, Ar and Kr gas mixtures are claimed to be perfect. The theoretical as well as the experimental α_T's by the CCF method as a function of $\bar{T}$ were however, used to estimate a' and b' and hence $\ln q_e$ at any intermediate temperature between 432K to 537K for each system. They are also shown in Fig. 8.2 by the dotted lines together with actual $\ln q_e$ at two available $\bar{T}$K.

The experimental α_T's by the existing method involved with CSF due to Maxwell and Slieker were also evaluated and shown in Figs. 8.3-8.5. The CSF due to L-J model can not be applied here as the cold wall temperature of the column was held fixed. The theoretical α_T's based on elastic collisions were also found out with the estimated ε_{ij}/k and σ_{ij} placed in Table 8.2 and shown in Figs. 8.3-8.5 only to see how far the elastic theory is now successful to

explain the experimental α_T's (Table 8.1) by the CCF and the existing method. The theoretical α_T's are placed in the last column of Table 8.1. Both the Tables 8.1 and 8.2, however, indicate the adequacy or otherwise of the CCF method to predict the actual and reliable α_T of such isotopic mixtures together with their correct force parameters from thermal diffusion.

8.2. Mathematical Formulations to Estimate Experimental α_T

In case of an ideal column of length *L*, both ends being closed, $\ln q_e$ of a gas mixture at any temperature $\bar{T}$ is given by[7,8]

$$\ln q_e = \frac{HL}{K_c + K_d} \qquad \text{..... (8.5)}$$

H, K_c and K_d are the functions of the transport coefficients of a gas mixture and are proportional to p^2,p^4 and p^0 respectively, *p* being the pressure in atmosphere. The above eq (8.5) thus becomes

$$\ln q_e = ap^2 / (b+p^4) \qquad \text{.....(8.6)}$$

But in case of actual column, parasitic remixing generally occurs. This can be taken into consideration by adding a term K_p, proportional to p^4 in the denominator of eq (8.5), $\ln q_e$ then becomes

$$\ln q_e = a'p^2/(b'+p^4) \qquad \text{..... (8.7)}$$

where *a'* and *b'* are related to *a* and *b* by :

$$a=a'(1+K_p/K_c) \text{ and } b=b'(1+K_p/K_c)$$

The above eq (8.7) can then be written as

$$p^2 / \ln q_e = b'/a' + (1/a')\, p^4 \qquad \text{.....(8.8)}$$

where a' and *b'* are two arbitrary constants which can be obtained from experimental $\ln q_e$ at different pressures *p* in atmosphere at a given temperature $\bar{T}$K.

Again, it has been found in Fig 8.2 that the experimental $\ln q_e$ increases with *p* and eventually becomes maximum at $p = (b')^{1/4}$ for which $\frac{\delta}{\delta p}(\ln q_e)=0$. The eq (8.7) then becomes

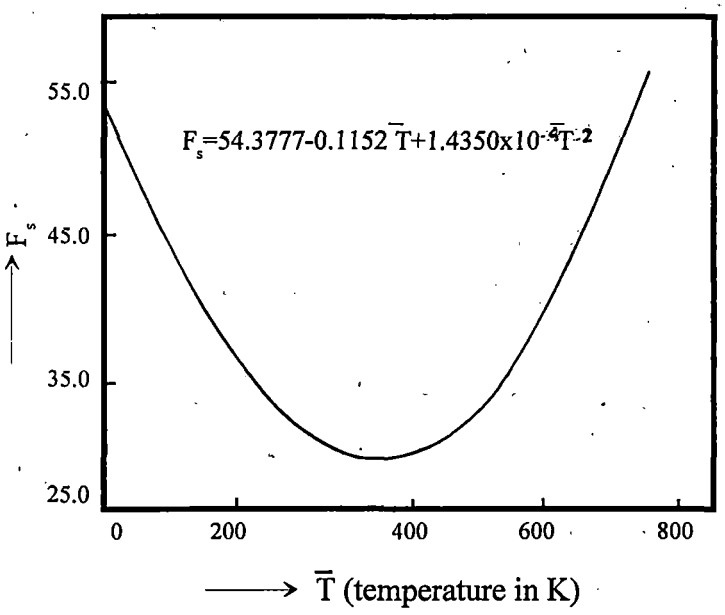

Fig. 8.1. Variation of column calibration factor F_s (CCF) against temperature in K

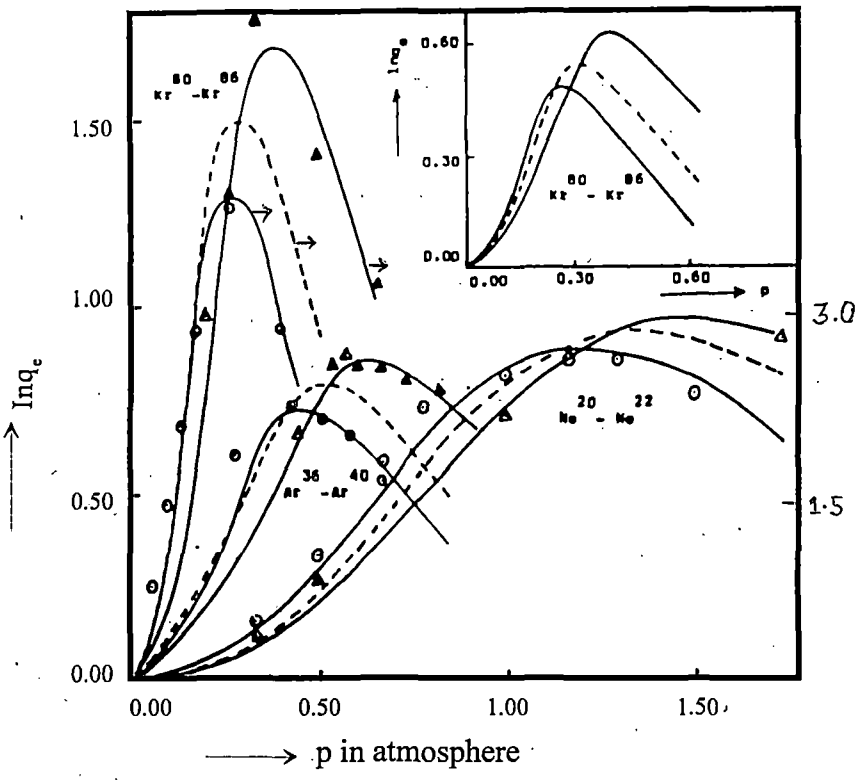

Fig. 8.2. i) Variation of Inq_e against p in atmosphere for Ne^{20}–Ne^{22}. -o-o- Experimental Inq_e at 447K, ----- Predicted In q_e at 492 K,-Δ-Δ- Experimental Inq_e at 537 K. (ii) Variation of Inq_e against p in atmosphere for Ar^{36}–Ar^{40}: -o-o- Experimental Inq_e at 432K, ----- Predicted Inq_e at 484.5 K, -Δ-Δ- Experimental Inq_e at 537 K. iii) Variation of Inq_e against p in atmosphere for Kr^{80}–Kr^{86}: -o-o- Experimental Inq_e at 447K, ----- Predicted Inq_e at 492K, -Δ-Δ- Experimental Inq_e at 537K. iv) Kr^{80}–Kr^{86} (Adjacent graph): ——— Adjusted Inq_e against p in atmosphere at 447K, ----- Predicted Inq_e against p in atmosphere at 492 K. —— Adjusted Inq_e against p in atmosphere at 537K.

$$\ln q_{max} = \frac{a'}{2\sqrt{b'}} \qquad \text{.....(8.9)}$$

With the known $\ln q_{max}$ in terms of a' and b' (Table 8.1) and F_s (Fig 8.1) of a given column[9], α_T of binary isotopic gas mixtures of Ne, Ar, Kr were found out from eq (8.1). They are placed in Table 8.1 and shown graphically in Figs 8.3-8.5.

One may obtain the experimental $\ln q_{max}$ from eq (8.5) which is also given by :

$$\ln q_{max} = \frac{HL}{2\sqrt{K_c K_d}} \qquad \text{..... (8.10)}$$

The exact expressions for H, K_c and K_d are given by:

$$\text{(i)} \quad H = \frac{2\pi}{6!}\left(\frac{\alpha_T \rho^2_{ij} g}{\eta_{ij}}\right) \cdot \frac{1}{2}(r_c + r_h)(r_c - r_h)^3 (2u)^2 h'$$

$$K_c = \frac{2\pi}{9!}(\rho^3_{ij} g^2 / \eta^2_{ij} D_{ij})_1 \frac{1}{2}(r_c + r_h)(r_c - r_h)^7 (2u)^2 k'_c$$

$$K_d = 2\pi(\rho_{ij} D_{ij})_1 \frac{1}{2}(r_c + r_h)(r_c - r_h) k'_d \qquad \text{.....(8.11)}$$

and

$$\text{(ii)} \quad H = C_1 = [S.F]_1 r_c^4 \left(\frac{\alpha_T \rho^2_{ij} g}{\eta_{ij}}\right)_1 \left(\frac{\Delta T}{\bar{T}}\right)^2$$

$$K_c = C_3 = [S.F]_3 r_c^8 (\rho^3_{ij} g^2 / n^2_{ij} D_{ij})_1 \left(\frac{\Delta T}{\bar{T}}\right)^2$$

$$K_d = C_2 = \pi(1-a^2) r_c^2 (\rho_{ij} D_{ij})_1 \qquad \text{..... (8.12)}$$

for Maxwell model and Slieker's model independent methods. The α_T in Maxwell model dependent and Slieker's model independent methods[15,16] could, however, be obtained by using eqs (8.10) to (8.12) in the following forms:

$$\alpha_T = (\text{Maxwell model}) = 2.39\,\frac{r_c - r_h}{L}\cdot\frac{\bar{T}}{\Delta T}\,\frac{\sqrt{k'_c k'_d}}{h'}\,\ln q_{max} \quad \ldots\ldots\ldots (8.13)$$

and

$$\alpha_T\,(\text{Slieker}) = 2.00\,\frac{r_c}{L}\,\frac{T}{\Delta T}\,\frac{\sqrt{\pi(1-a^2)[S.F]_3}}{[S.F]_1}\,\ln q_{max} \quad \ldots\ldots\ldots (8.14)$$

The symbols h', k_c', k'_d and $[S.F]_1$, $\pi(1-a^2)$, $[S.F]_3$ are dimensionless CSF due to Maxwell and Slieker respectively ρ_{ij} is the mass density of the gas mixture of coefficient of viscosity η_{ij} and diffusion coefficient D_{ij}, $u = \frac{T_h - T_c}{T_h + T_c}$, $\Delta T = T_h - T_c$ and g is the acceleration due to gravity.

The α_T's thus evaluated from eqs. (8.13) and (8.14) due to Maxwell model and Slieker's CSF respectively are placed in Table 8.1. They are also shown in Figs. 8.3-8.5 for Ne^{20}-Ne^{22}, Ar^{36}-Ar^{40} and Kr^{80}-Kr^{86} mixtures in order to compare them with the theoretical α_T computed with their respective ε_{ij}/k and σ_{ij}.

8.3. Theoretical Elastic α_T together with Force Parameters ε_{ij}/k and σ_{ij}.

According to gas kinetic theory the theoretical α_T based on elastic collisions[1] is

$$\alpha_T = g(6C^*_{ij} - 5) \quad \ldots\ldots\ldots (8.15)$$

where

$$g = \frac{1}{6[\lambda_{ij}]_1}\,\frac{S^{(i)}x_i - S^{(j)}x_i}{X_\lambda + Y_\lambda}$$

is a complicated function of composition and thermal conductivities of a gas mixture. The temperature dependence of α_T is mainly governed by $(6C^*_{ij}-5)$ which involves with like or unlike interactions. The experimental α_T as a function of $\bar{T}$ is[17]

$$(\alpha_T)_{expt} = A + B / \bar{T}. \quad \ldots\ldots\ldots (8.16)$$

Although g is a slowly varying function of $\bar{T}$, we may assume to be a temperature

Table 8.1. Experimental and theoretical thermal diffusionfactor α_T of binary isotopic mixtures of Neon, Argon and Krypton with temperatures in K.

Column used	System	Hot Wall Temp. (T_h) in K.	Cold Wall Temp. (T_c) in K.	Mean Temp. in K $T=\frac{T_h+T_c}{2}$	a' $(atm)^2$	b' $(atm)^4$	Computed $\ln q_{max}$ from eq (8.9)	Column calibration factor (F_c)
L=Length of the column. =182.0 cm.	Ne^{20}–Ne^{22}	596	298	447	2.5470	2.0188	0.8963	31.5599
		656	328	492	3.3670	3.3025	0.9264	32.4355
		716	358	537	4.3365	4.9660	0.9730	33.9012
Hot Wall radius r_h = 0.0254 cm.	Ar^{36}–Ar^{40}	576	288	432	0.2942	0.0415	0.7221	31.3957
		646	323	484.5	0.4149	0.0701	0.7836	32.2485
		716	358	537	0.7037	0.1683	0.8577	33.9012
Cold Wall radius r_c = 0.635 cm.	Kr^{80}–Kr^{86}	596	298	447	0.5342	0.0046	3.9382	31.5599
					0.0653	0.0046	0.4814	
		656	328	492	0.7963	0.0078	4.5082	32.4355
					0.0973	0.0078	0.5511	
		716	358	537	1.5540	0.0231	5.1123	33.9012
					0.1900	0.0231	0.6250	

Column used	System	Estimated α_T using			Computed theoritical α_T
		Present method	Maxwell's shape factor	Slieker's shape factor	
L=Length of the column =182.0 cm.	Ne^{20}–Ne^{22}	0.0284	0.0156	0.0179	0.0294
		0.0286	0.0161	0.0185	0.0298
		0.0287	0.0169	0.0195	0.0297
Hot Wall radius r_h = 0.0254 cm.	Ar^{36}–Ar^{40}	0.0230	0.0126	0.0144	0.0259
		0.0243	0.0136	0.0156	0.0268
		0.0253	0.0149	0.0171	0.0277
Cold Wall radius r_c = 0.635 cm.	Kr^{80}–Kr^{86}	0.1248	0.0684	0.0785	0.0135
		0.0153			
		0.1390	0.0783	0.0899	0.0157
		0.0170			
		0.1508	0.0888	0.1019	0.0170
		0.0184			

independent one. C^*_{ij} may be expressed as a function of reduced temperature $\bar{T}^*$ like

$$C^*_{ij} = C + D/\bar{T}^* \qquad \text{.....(8.17)}$$

where

$$\bar{T}^* = \bar{T}/(\varepsilon_{ij}/k).$$

The above eq (8.15) thus becomes

$$(\alpha_T)_{theor.} = (6C - 5)g + 6gD/T^* \qquad \text{.....(8.18)}$$

where C and D are new constants. Comparing eqs. (8.16) and (8.18) one may get

$$g=A/(6C-5)$$

From the fitted equations of $(\alpha_T)_{expt}$ against $1/\bar{T}$, A and B were first evaluated. Similarly C^*_{ij} reported elsewhere[18] for (12-6) L-J potential was plotted against $1/\bar{T}^*$ to get C and D of eq (8.17)

Thus 'g' along with $(\alpha_T)_{expt.} = (6C^*_{ij} - 5)g$ fixes C^*_{ij} and hence $\bar{T}^*$ to estimate ε_{ij}/k of the respective molecule.

With the value of ε_{ij}/k first estimated, one may repeat the total procedure as mentioned above, to get more correct ε_{ij}/k in order to present them in Table 8.2. They are found in good agreement with the available literature values. Reported viscosity data are then used with the estimated ε_{ij}/k to get the molecular diameter σ_{ij} as shown in Table 8.2. The theoretical α_T's for Ne^{20}- Ne^{22}, Ar^{36}-Ar^{40} and Kr^{80}-Kr^{86} were then evaluated with those ε_{ii}/k, ε_{jj}/k and ε_{ij}/k (Table 8.2) and shown in Figs. 8.3-8.5 respectively.

8.4. Results and Discussions

The least square fitted euqations of $p^2/\ln q_e$ against p^4 from the available $\ln q_e$ vs p in atmosphere[9] as illustrated graphically in Fig. 8.2, were worked out for 9.7% of Ar^{36} in Ar^{40}, Ne^{20}-Ne^{22} and Kr^{80}-Kr^{86}, the latter two with their natural isotopic abundances, at two experimental temperatures. The pressure

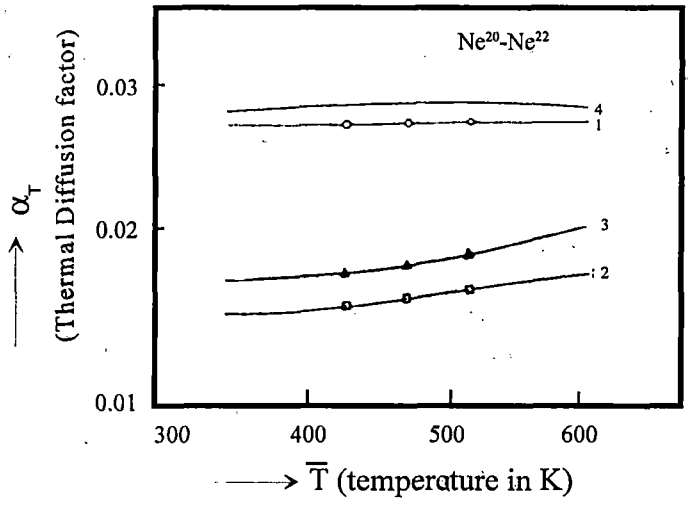

Fig. 8.3. Plot of α_T's against $\overline{T}$ in K for Ne^{20}–Ne^{22}. -o-o- Curve 1:Experimental α_T from F_s and Inq_{max}. -□-□- Curve 2: Experimental α_T from Maxwell's shape factors. -Δ-Δ- Curve 3: Experimental α_T using Slieker's shape factors. —— Curve 4: Theoretical α_T based on elastic collision.

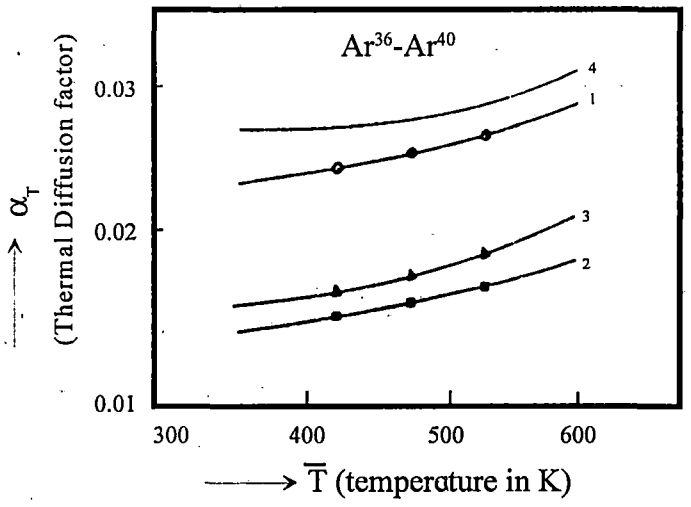

Fig. 8.4. Plot of α_T's against $\overline{T}$ for Ar^{36}–Ar^{40}. -O-O- Curve 1:Experimental α_T from F_s and Inq_{max}. -□-□- Curve 2: Experimental α_T from Maxwell's shape factors. -Δ-Δ- Curve 3: Experimental α_T using Slieker's shape factors. —— Curve 4: Theoretical α_T based on elastic collision.

dependence of $\ln q_e$ at any intermediate temperature for them, as shown by dotted lines in Fig. 8.2, were also inferred from $\ln q_{max}$ in terms of known F_s and α_T assuming the linear relationship of (b'/a') with $\bar{T}$ for the three aforesaid mixtures. $p^2/\ln q_e$ as a linear function of p^4 are, however, expressed by the following equations for;

i) Ar^{36}-Ar^{40} (with 9.7% of Ar^{36} in Ar^{40})

$p^2/\ln q_e = 0.1411 + 3.3990p^4$ at 432 K

$p^2/\ln q_e = 0.1690 + 2.4102p^4$ at 484 K

$p^2/\ln q_e = 0.2392 + 1.4210p^4$ at 537 K

ii) Ne^{20}-Ne^{22} (with natural isotopic abundances)

$p^2/\ln q_e = 0.7926 + 0.3926p^4$ at 447 K

$p^2/\ln q_e = 0.9808 + 0.2970p^4$ at 492 K

$p^2/\ln q_e = 1.1452 + 0.2306p^4$ at 537 K

and for Kr^{80}- Kr^{86} (with natural isotopic abundances)

$p^2/\ln q_e = 0.0086 + 1.8720p^4$ at 447 K

$p^2/\ln q_e = 0.0098 + 1.2558p^4$ at 492 K

$p^2/\ln q_e = 0.0149 + 0.6435p^4$ at 537 K.

But $\ln q_{max}$ of Krypton, estimated from the measured values of $\ln q_e$ as a function of pressure (Fig. 8.2) in terms of a' and b' (Table 8.1) is found to be 8.18 times larger than the widely reported data elsewhere.[7] Adjustment of $\ln q_e$ is, therefore, necessary to get actual α_T's of Kr^{80}-Kr^{86}, as shown by curve 5 in Fig. 8.5, from the follwoing $p^2/\ln q_e$ against p^4 relations :

$p^2/\ln q_e = 0.0704 + 15.3139p^4$ at 447 K

$p^2/\ln q_e = 0.0802 + 10.2775p^4$ at 492 K

$p^2/\ln q_e = 0.1216 + 5.2632p^4$ at 537 K.

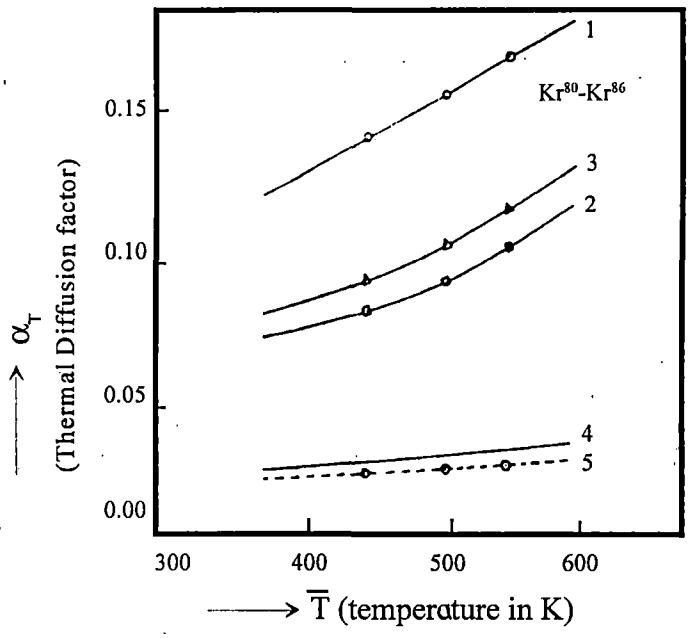

Fig. 8.5. Plot of α_T's against $\overline{T}$ for Kr^{80}–Kr^{86}: -O-O- Curve 1:Experimental α_T from F_s and Inq_{max}, -□-□- Curve 2: Experimental α_T from Maxwell's shape factors, -Δ-Δ- Curve 3: Experimental α_T using Slieker's shape factors, —— Curve 4: Theoretical α_T based on elastic collision, –o–o– Curve 5: Experimental α_T from F_s and adjusted Inq_{max}

Table8.2. Maxwell's model dependent and slicker's model independent column shape factors, (CSF) coefficient of viscosity together with estimated force parameters ϵ_{ij}/k and molecular diameter σ_{ij} used in the calculation of α_T of simple isotopic gas mixtures.

System	Model potential	Estimated		Reported		Mean Temp. (T) in K
		ϵ_{ij}/k in K	σ_{ij}/k in Å	ϵ_{ij}/k in K	σ_{ij} in Å	
Ne^{20}-Ne^{22}	LJ 12-6	40.77	3.1840	41.19*	3.074*	417
						492
				27.50**	2.858**	537
Ar^{36}-Ar^{40}	LJ 12-6	118.41	3.9543	125.20*	3.405*	432
						484.5
				119.50**	3.826**	537
Kr^{80}-Kr^{86}	LJ 12-6	202.41	4.1689	199.20*	4.020*	417
						492
				166.70**	4.130**	537

System	Model potential	Column shape factors (CSF)						$\eta_{ij} \times 10^5$ gm × cm^{-1} × sec^{-1}
		Maxwell			Slicker			
		k'	k'_c	k'_d	$[S \cdot F]_1 \times 6!$	$\pi(1-a^2)$	$[S \cdot F]_3 \times 9!$	
Ne^{20}-Ne^{22}	LJ 12-6	0.815	1.760	0.790	0.937	3.137	0.711	31.40
								33.35
								35.17
Ar^{36}-Ar^{40}	LJ 12-6	0.815	1.760	0.790	0.937	3.137	0.711	21.80
								23.95
								26.10
Kr^{80}-Kr^{86}	LJ 12-6	0.815	1.760	0.790	0.937	3.137	0.711	25.50
								28.15
								30.80

*Maitland *et al.* (1981)
**Hirchfelder *et al.* (1964)

The new $\ln q_e$ against p in atmosphere is shown by the adjacent curves in Fig. 8.2. The corresponding $\ln q_{max}$'s are placed in Table 8.1 together with those obtained from $\ln q_e$ vs p measured by Moran and Watson[9]. The $\ln q_{max}$'s for all the isotopic molecular mixtures were, however, determined from eq. (8.9) with a' and b' governing their pressure variation of $\ln q_e$ as shown in Fig. 8.2. They are placed in the 8th column of Table 8.1.

Since F_s is supposed not to depend on molecular model we therefore, estimated three values of F_s from eq. (8.1.) for this column[9] through the measured $\ln q_{max}$ and reliable α_T's from the other sources[10] for Ar^{36}-Ar^{40} at 432 K, 537K and Ne^{20}-Ne^{22} at 447K respectively. It is interesting to note in Fig. 8.1, that the temperature varition of F_s is the same as observed earlier[5-6] only the coefficients of $\bar{T}$ and $\bar{T}^2$ are slightly different. Although r_c/r_h (=25) for the present column is too large, the temperatue variation of F_s is found to be concave in nature.

The magnitudes and trends of α_T with respect to temperature $\bar{T}$ could, now be obtained for Ne^{20}-Ne^{22}, Ar^{36}-Ar^{40} and Kr^{80}-Kr^{86} from eq. (8.1) in terms of $\ln q_{max}$ and F_s. The expected close agreement of α_T's from the CCF method with theoretical ones might express the reliability of F_s and the model independency of CCF method may once again be confirmed. The α_T's by the CCF method are placed in the 10th column of Table 8.1. The variation of these α_T's with $\bar{T}$ are shown graphically in Figs. 8.3.-8.5 for Ne^{20}-Ne^{22}, Ar^{36}-Ar^{40} and Kr^{80}-Kr^{86} respectively by the curve No.1.

In order to ensure the reliability of the temperature dependence of α_T the molecular force parameters ε_{ij}/k and σ_{ij} were also detemined by using eq (8.18) and the available coefficients of viscosity respectively. The estimated ε_{ii}/k or ε_{jj}/k and σ_{ii} or σ_{jj} of the isotopic gases are placed in the 3rd and the 4th columns of Table 8.2. The close agreement of them with the literature values at once suggests the technique to estimate α_T is really accurate and reliable. The experimental α_T's were also computed from eqs (8.13) and (8.14) by using Maxwell's inverse fifth power potential and Slieker's model independent column shape factors (CSF) which are placed in Table 8.2. These α_T's are placed in

the 11th and the 12th columns of Tables 8.1 respectively. The variation of these α_T's with $\bar{T}$ are also shown graphically by curves 2 and 3 respectively in Figs 8.3-8.5. The α_T's as shown in Figs 8.3-8.5, due to Maxwell and Slieker's methods agree excellently with α_T's by the CCF method so far their trends with $\bar{T}$ are concerned, although the magnitude of α_T by the present method is higher.

The existing frame work of derivation of eqs. (8.13) and (8.14) are really very interesting. The formulations so derived show that the molecular model appears in them through CSF which seems to be an important stepforward in the existing method based on Furry[2] and Jones[4] column theory.

With the estimatd force parameters ε_{ij}/k and σ_{ij}, presented in Table 8.2, theoretical α_T's based on the elastic collisions were also evaluated and placed in the 13th column of Table 8.1 The variation of theoretical α_T's with $\bar{T}$ are shown graphically by curve 4 in each of the Figs. 8.3-8.5 for Ne^{20}-Ne^{22}, Ar^{36}-Ar^{40} and Kr^{80}-Kr^{86} respectively. The α_T's due to elastic collision theory are found to be almost of the same magnitude with those by the CCF method. Besides all these, it is seen that the trends of α_T's with respect to temperature by the present CCF method agree excellently well with the theoretical one in all the systems.

From the discussions made above, it is confirmed that F_s is a molecular model independent parameter. F_s is further, claimed to be a perfect, simple and straightforward one to locate the magnitude and trend of α_T with respect to $\bar{T}$. Moreover, α_T against $1/\bar{T}$ may be considered as a simple and useful technique in determining the exact force parameter of molecules too, to observe the temperature dependence of α_T of any binary isotopic and nonisotopic gas mixture.

8.5. Conclusion

Model independency of CCF, F_s is now once again established in determining the reliable α_T's of any binary gas mixture in column measurements. It is, therefore, desirable to study more TD columns of different column

geometries to arrive at the functional relationship of F_s with r_c, r_h L and $\bar{T}$ with the experimentally determined lnq_{max} and α_T of interesting pair of molecules. The simultaneous estimation of α_T's and F_s with the corresponding force parameters from α_T vs $1/\bar{T}$ seems to be an important stepforward to test the applicability of F_s. Furthermore, the very existence of inelastic collisions among the molecules in the process of thermal diffusion might be detected and improved with certainty through such rigorous study.

References

[1] S. Chapman and T.G. Cowling : *The Mathematical Theory of Non Uniform Gases (*Cambridge University Press, NY, 1952).

[2] W. H. Furry and R.C. Jones : Phys. Rev. **69** (1946) 459.

[3] J. L. Navarro, J. A. Madariage and J.M. Saviron : J. Phys. Soc. Jpn. **50** (1983) 1603.

[4] R. C. Jones and W.H. Furry. : Mod. Phys. **18** (1946) 151.

[5] S. Acharyya, I. L. Saha, A. K. Datta and A. K. Chatterjee : J. Phys. Soc. Jpn. **56** (1990) 3602.

[6] A. K. Datta, G.Dasgupta and S. Acharyya : J. Phys. Soc. Jpn. **59** (1990) 3602.

[7] A. K. Datta and S. Acharyya : J. Phys. Soc. Jpn. **62** (1993) 1527.

[8] G. Dasgupta, A. K. Datta and S. Acharyya : Pramana J. Phys., India, **43** (1994) 81.

[9] T. I. Moran and W.W. Watson : Phys. Rev. **111** (1957) 103.

[10] F. Vandervolk : Ph. D. Dissertation, 1963.

[11] R. Paul, A. J. Howard and W.W. Watson : J. Chem. Phys. **39** (1963) 3053.

[12] H. Brown : Phys. Rev. **58** (1940) 661.

[13] B. N.Srivastava and K. P. Srivastava : Physica **23** (1957) 103.

[14] B. N. Srivastava and M.P. Madan : Proc. Phys. Soc. London **66** (1953) 277.

[15] G. Vasaru : *Thermal Diffusion Column,* supplied by S. Raman (B.A.R.C., Bombay).

[16] C. J. G. Slieker : Z. Naturforsch. **20** (1965) 591.

[17] G. Dasgupta, N. Ghosh, N. Nandi, A.K. Chatterjee and S. Acharyya: J. Phys. Soc. Jpn. **65** (1996) 2506.

[18] M. Klein and F.J. Smith : Tables of collision integral for the (m, 6) potential for the values of m, Arnold Engineering Development Centre, Tennessee, 1968.